inter.noise 2014
MELBOURNE AUSTRALIA
16-19 NOVEMBER

Transformation of sound by a phononic crystal

Nicolas COTE[1]; Jérôme VASSEUR[2]; Quentin SOURON[1]; Anne-Christine HLADKY-HENNION[1]

[1] IEMN, UMR 8520 CNRS, ISEN Department, 41 Boulevard Vauban, 59046 Lille, France

[2] IEMN, UMR 8520 CNRS, Cité Scientifique, 59652 Villeneuve d'Ascq Cedex, France

ABSTRACT

Several noise barriers made of phononic crystals (i.e. manmade composite materials with a periodic structure) have been designed over the last decade. The periodic structure of phononic crystal avoids sound propagation in a defined frequency range called Bragg band gap (i.e. waves are evanescent). This study aims at quantifying the perceptual impact of a noise barrier based on a phononic crystal in terms of noise annoyance attenuation. First, a specific phononic crystal has been designed to study timbre modifications. Then, a combined acoustics/auditory analysis of noise barrier made of a phononic crystal is employed. The acoustic analysis consists in numerical simulations and measurements of acoustical scenes. In addition, several psychoacoustics parameters are estimated from the synthesized/recorded acoustic signals. In details, two specific timbre features are studied: the spectrum and temporal modifications of the sound source.

Keywords: Noise barrier, Phononic crystal I-INCE Classification of Subjects Number(s): 31.1, 63.2

1. INTRODUCTION

Noise is an important source of annoyance and considered as a key factor on public health. Noise has multiple effects on human general state of health (1): both psychological like stress or a lack of concentration and physiological like sleep disturbances or cardiovascular changes. In particular, noise can aggravate serious pre-existent physiological disorders. At the European level, the European Parliament adopted on June 25th 2002 directive 2002/49/CE to lay the basis for the fight against environmental noise (2). This European directive has three main objectives: to carry out strategic noise maps (with the same acoustic indicators, L_{DEN} and L_{Night}, for the 25 European states), to inform the public, and to implement action plans at local level.

With the aim of reducing the resident noise exposure, the contracting authorities (state, regional authorities) can place noise barriers along ring roads, highways and railways, between the noise sources and the exposed environments. However, such barriers are substantial architectural elements that can decrease landscape quality. Most of them employ non sustainable materials like concrete, metal or plastic, and have a limited acoustical effect due to the reduced geometrical shadow zone behind the barrier produced by the diffraction of acoustic waves on the barrier top edge (3). Barriers reduce the mortality of the small wildlife populations whereas they exacerbate the habitat fragmentation effect of roads in particular on small animals (4). Moreover, these noise barriers are basically continuous walls that has a negative visual impact, reduce sunlight for the surrounding residents and have a significant resistance to the flow of air.

Within the last ten years, several studies described the acoustical effects introduced by Phononic Crystals (PC) (5, 6). PCs are artificial materials (or structured materials) made of periodic distributions of inclusions inserted in a matrix. Due to their periodic structure, PCs may present, under certain conditions (geometry of the array of inclusions, filling factor of inclusions, inclusion shape ...), band-gaps where the propagation of acoustic waves is forbidden. Such band gaps are either absolute, i.e. the waves are evanescent whatever the incidence angle (called Absolute Band Gap, ABG) or for some specific angle, for example the normal incidence (named Band Gap 0°, BG 0°).

This spectral property confers to PCs potential applications in various fields such as sound insulation, selective frequency filtering, or for the realization of more powerful transducers for nondestructive control, medical imaging, etc. For PC applications in the audible frequency range for traffic noise, various authors (7, 8) have considered periodic distributions of rigid solid scatterers placed in the air background. However, PC-based noise barriers attenuate a sharp frequency band compared to the wideband noise emitted by cars and

[1] nicolas.cote@isen.fr

trucks. Therefore, researchers introduced several noise control elements in such barriers: scatterers, resonators and absorptive materials. An example of such a PC-based noise barrier has been developed by Romero-Garcia et al (9): the scatterers are covered by 4 cm of porous material and are slotted along its entire length. This system called Sonic Crystal Acoustic Barrier (SCAB) achieved 8 dB to 11 dB in absorption and 15 dB to 24 dB in insulation (see the EN-1793 standards). Koussa et al (10) has proposed to combine a free-standing noise barrier and a PC-based noise barrier with two lattice constants (8.5 cm and 17 cm). This association increases the acoustic insulation by 2 to 6 dB (depending on the traffic configuration) of the free-standing noise barrier alone. In a similar way but based on natural material, Lagarrigue et al (11) introduced hollow bamboos as elements of the crystal. They made a hole in each node of the bamboos to create resonator cavities. Such resonators enable a significant attenuation of noise at frequencies around 340 Hz.

Another phenomenon called negative refraction is associated to PCs. This occurs when the dispersion curves of the periodic structure present branches with negative slope. In this case, the sound "ray" at the interface between the PC and its surrounding medium, is refracted with a negative angle. In other words, in the frequency range of the band with negative slope, the PC behaves as an effective medium with negative index of refraction. Moreover, when the absolute value of the index of refraction of the PC is equal to that of the surrounding medium for all incidence angles, one may observe focusing of the waves (all angles negative refraction criterion): a point source located in front of one side of a PC-based barrier gives a point image at the other side of the barrier. The distance between the point source and the point image is twice as large as the PC barrier (12, 13), see Figure 1

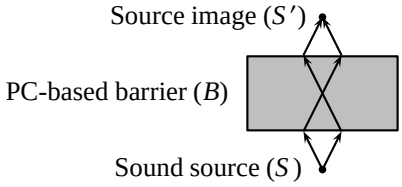

Figure 1 – Negative refraction effect: the sound source (S) in front of the PC-based noise barrier creates a source image (S').

To the best of our knowledge one paper only describes the perceptive effects of PC-based noise barriers. Spiousas et al (14) studied the influence of a PC on the auditory distance perception of sound sources. The results of their auditory test show that negative refraction in PCs may artificially bring a sound source closer to the listener.

This paper presents a combined acoustical/perceptual study of a noise barrier made of a PC. It is divided in four sections. Section 2 describes the studied PC and the protocol employed to evaluate the noise barrier. Section 3 presents the results of the numerical computations whereas Section 4 presents the results of the experiments. The last section (Section 5) analyses the estimated psychoacoustic parameters of the PC-based noise barrier.

2. METHOD

This paper aims at analyzing whether a noise barrier made of a phononic crystal introduces audible effects such as spectrum and temporal modifications. Such modifications may affect the timbre of a sound source. For this purpose a specific PC with three effects in the audible frequency range has been designed. These three phenomena are:

- a band gap at normal incidence (BG 0°),
- an absolute band gap (ABG),
- a frequency range where negative refraction occurs.

Each phenomenon and associated audible effects are quantified with the use of both acoustic and perceptual parameters. This specific PC is composed of rigid (filled) cylinders of radius $r = 5$ cm arranged according to a triangular lattice with lattice parameter $a = 12$ cm (see figure 2). This study employs the following approach:

- a description of the PC and an analysis of the dispersion curves that shows the three phenomena introduced above,
- a theoretical and an experimental studies of the PC-based noise barrier, for several sound scenes described in Table 1, using
  - numerical computations based on the finite element method,

– acoustical measurements,
- the synthesis of a sound database based on the derived impulse responses for each sound scene and reference sound files,
- a perceptual analysis of the impulse responses and the sound database based on several psychoacoustic features.

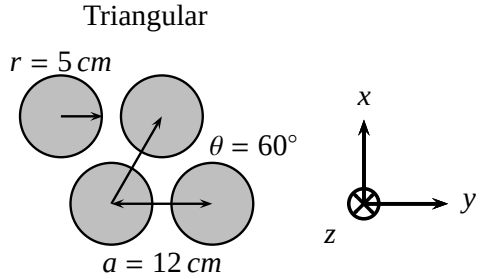

Figure 2 – Description of the phononic crystal designed for this study (with associated axes).

3. NUMERICAL ANALYSIS

3.1 Dispersion curves

The dispersion curves are computed with the finite element method using the ATILA software (15). Since the cylinders are considered as uniform and infinite in the z direction, a 2D mesh is employed only. First, a single scatterer is meshed, composed of several elements connected by nodes where periodical boundary conditions are imposed (16). Quadratic interpolation elements are considered in the computation. The cylinders are assumed as rigid and placed in air. Density and speed of sound in air are $\rho_{\text{air}} = 1.3\,\text{kg}\,\text{m}^{-3}$ and $c_{\text{air}} = 339\,\text{m}\,\text{s}^{-1}$, respectively. The dispersion curves are presented in Figure 3. We observe the three phenomena detailed below.

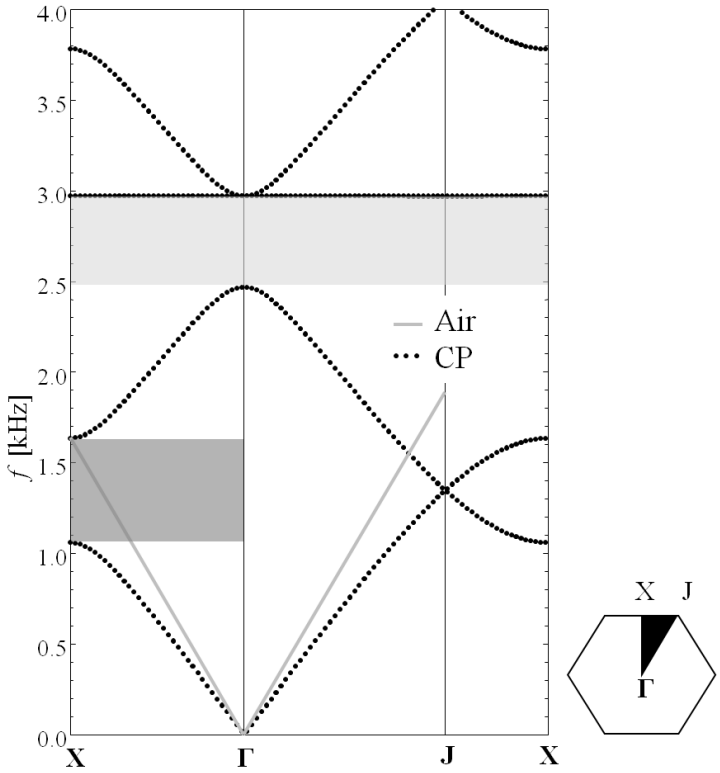

Figure 3 – Dispersion curves of the phononic crystal designed for this study (including the Brillouin zone).

- In the direction ΓX (0°, normal incident), we observe a band gap in the frequency range 1080 Hz to 1610 Hz (in dark gray on Figure 3). The band gap (BG 0°) is not absolute since it is not observed in this frequency range along the other directions of propagation ΓJ and JX).

- At higher frequencies, in the range 1610 Hz to 2500 Hz, the dispersion curves exhibit branches with negative slope. The straight lines corresponding to the celerity in air cross these bands at two slightly different frequencies along the principal directions of propagation namely at 1620 Hz along ΓX and 1550 Hz along ΓJ. That means that the effective index of refraction of the PC is not strictly equal to that of air in the ΓX and ΓJ directions. However, some focusing effect is expected even though the PC is not strictly isotropic.
- At even higher frequencies, in the range 2500 Hz to 2960 Hz, no propagation mode exists. In this absolute band gap (ABG) the propagation of acoustic waves is forbidden whatever the incident direction.

3.2 Harmonic analysis of the PC-based noise barrier in free-field

Since we observed these three effects in the audible frequency range for the phononic crystal, we now would like to observe the same effects on a noise barrier made of this PC. For this purpose we designed a barrier composed of 5 rows of 11/12 cylinders. The mesh includes the barrier and a large region of air around the barrier. An ideal point source (S) is placed at 0.05 m of the barrier and in front of a cylinder ($y = 0$ cm, see Figure 4). The ATILA finite element code is employed to predict the acoustic pressure (p) around the PC-based noise barrier. Figure 5 shows the pressure field for three different frequencies: 1300, 1700 and 2700 Hz. Each figure shows one phenomenon described in the above sub-section. Figure 5a shows the band gap in the ΓX direction (BG 0°): the acoustic pressure is relatively low along the x line (see Figure 4) whereas the pressure increases in the oblique directions behind the barrier. Figure 5b shows the source image due to the negative refraction and the focusing effect. Figure 5c shows the absolute band gap (ABG): the pressure is very low in all directions behind the barrier.

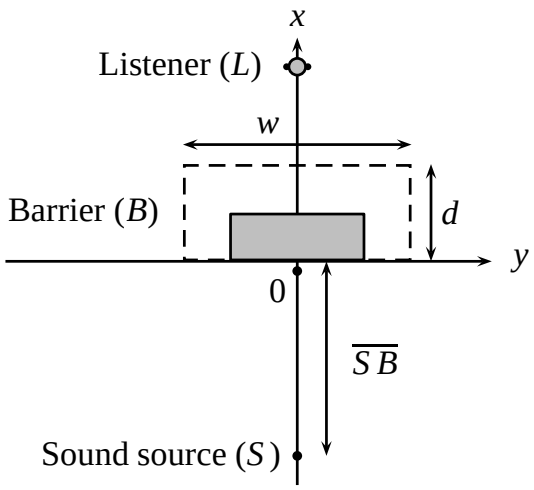

Figure 4 – Position of the sound source (S), the noise barrier (B) and the pseudo-listener (L) for the different sound scenes described in Table 1.

To precisely localize the image point, the pressure field (p) along the x line (see Figure 4) behind the barrier and for the frequency range 1400 Hz to 2000 Hz has been analyzed. This line is perpendicular to the barrier and pass through the sound source (S) and through the focusing area ($y = 0$ cm). The results show that the acoustic pressure is maximal for frequencies around 1700 Hz and at 60 cm behind the barrier. The distance between the sound source and the image point is close to twice the barrier depth (1.166 m instead of 1.032 m) indicating that the all angles negative refraction criterion is nearly satisfied.

3.3 Harmonic analysis of noise barriers with a pseudo-listener

The simulation applied in Section 3.2 is repeated but with a pseudo-listener placed at 150 cm behind the barrier, i.e. about 90 cm beyond the image point. We use a cylinder with a radius $r' = 10$ cm as a model for the listener. Figure 4 presents the position of the sound source (S), the noise barrier (B) and the "pseudo"-listener (L) for all sound scenes listed in Table 1. The sound source and the listener are placed on each side of the barrier. To quantify the performance of the PC-based barrier, three types of simulations are computed:

- in free-field: there is no obstacle between the sound source and the pseudo-listener (sound scenes 1 and 2),
- with the PC-based noise barrier described in Section 3.2 placed on the gray area (sound scenes 3 to 6),
- with the free-standing noise barrier (consider rigid) that has the same depth and width as the PC-based barrier (sound scenes 7 to 10).

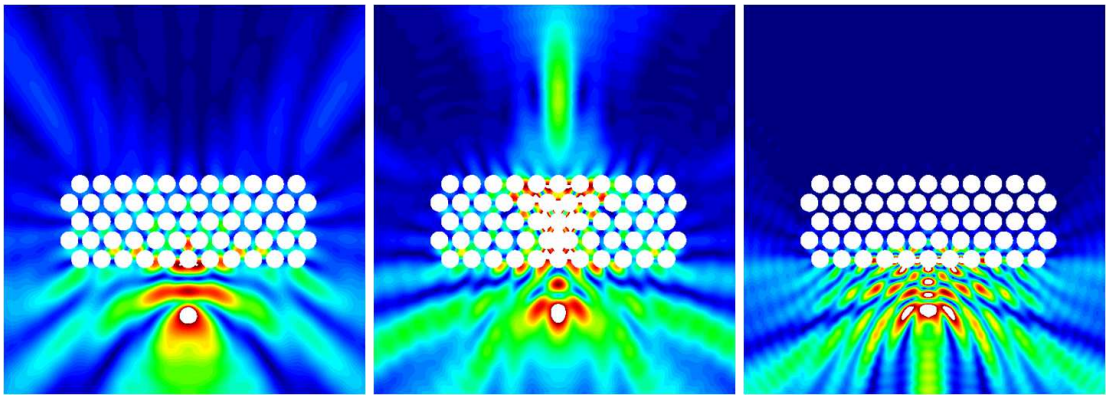

(a) $f = 1300\,\text{Hz}$ (b) $f = 1700\,\text{Hz}$ (c) $f = 2700\,\text{Hz}$

Figure 5 – Theoretical pressure field for three different frequencies.

Table 1 – List of the 10 sound scenes.

Num.	*Barrier type*	$\overline{SB}$ [m]	w [m]	d [m]
1	-	2	-	0.5
2	-	0.05	-	0.5
3	PC-based	2	1.4	0.5
4	PC-based	2	2.35	0.5
5	PC-based	2	1.4	1
6	PC-based	0.05	1.4	0.5
7	free-standing	2	1.4	0.5
8	free-standing	2	2.35	0.5
9	free-standing	2	1.4	1
10	free-standing	0.05	1.4	0.5

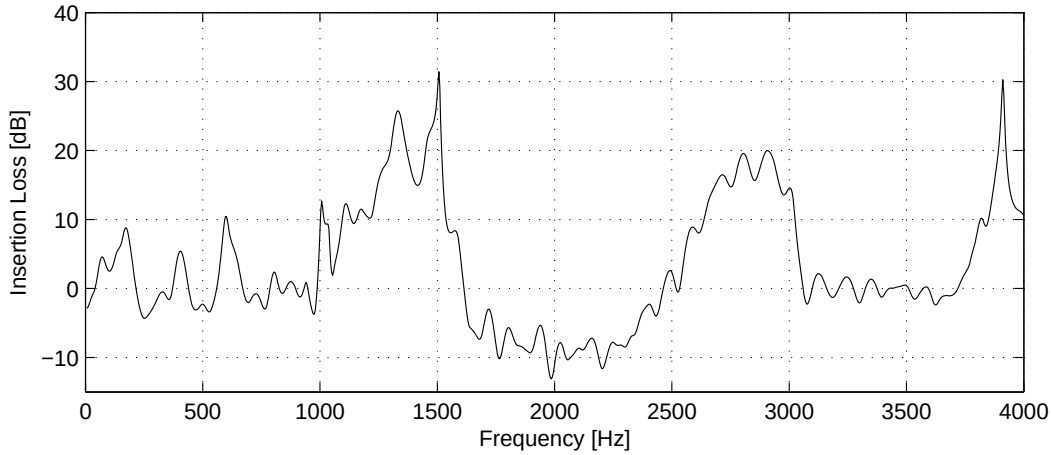

Figure 6 – Insertion Loss (IL) introduced by the PC-based noise barrier for the signal obtained at the left “ear” of the pseudo-listener.

The harmonic analysis is applied in the frequency range 7.81 Hz to 4000 Hz, with a step of 3.9 Hz (i.e. 1024 points). Both real and imaginary parts of the acoustic pressure p is predicted on each "ear" of the pseudo-listener (left and right sides of the cylinder). They simulate the acoustic signals received at the *Ear Reference Point* (ERP) according to the classification of the International Telecommunication Union (ITU) (17). An inverse Fourier transform is applied to obtain the 256 ms impulse response for each sound scene of Table 1 (with a sampling frequency $F_S = 8000$ Hz). The harmonic analysis is presented through the Insertion Loss (IL) defined as the difference at the listener left "ear" of the pseudo-listener between the spectrum with and without the system under study. Thus, a positive value corresponds to an attenuation of the pressure level at the left "ear" of the pseudo-listener. Figure 6 shows the IL introduced by the PC-based noise barrier (sound scene 6 of Table 1) compared to the respective free-field case (sound scene 2). The IL shows an attenuation around 15 dB of the acoustic wave introduced by the PC-based barrier in the band gap 1080 Hz to 1610 Hz (BG 0°) and in the absolute band gap 2470 Hz to 2960 Hz (ABG). Even though the pseudo-listener is placed behind the source image, we observe an amplification (up to 12 dB) of the sound level in the frequency range of the negative refraction, i.e. 1610 Hz to 2500 Hz.

4. EXPERIMENT

4.1 Protocol

To check the theoretical predictions obtained with the finite element method, we carried out an experiment with a demonstrator of our PC-based noise barrier. We manufactured the barrier described in Section 3.2: 57 hollow cylinders arranged in 5 rows of 11/12 cylinders ($w = 1.4$ m and $d = 0.5$ m) with a period of the triangular lattice $a = 12$ cm. The cylinders (in PVC) have an outer radius $r = 5$ cm and a thickness $\delta_r = 2$ mm. The choice of hollow cylinders rather than filled ones does not influence the experimental results because inclusions are surrounding with air (7). The tubes of length $l = 200$ cm are fixed at one end on a large slab (in plywood) with the other end remaining free, see Figure 7. A *Gallien Krueger* 410RBH loudspeaker amplified by a *B& K* type 2716 audio power amplifier connected to a *Roland Quad Capture* sound card is employed to produce the incoming acoustic wave. The transmitted wave is recorded by a *Sennheiser* MKE2-P-C microphone connected to the same sound card. Here, no dummy head for binaural recording was employed. A sampling frequency of $F_S = 48$ kHz was used. The incoming signal is a logarithmic sweep-sine of 5 seconds between 100 and 4000 Hz repeated 10 times to reduced the background noise. The measurements are conducted in free-field (sound scenes 1 and 2) and with the PC-based barrier (sound scenes 3 and 6).

Figure 7 – Picture of the demonstrator of our PC-based noise barrier.

Figure 8 shows the measured and predicted Insertion Loss introduced by the PC-based noise barrier (sound scene 6 of Table 1) compared to the respective free-field case (sound scene 2). Since the loudspeaker is 61 cm wide and the numerical computation considers an isolated sound source, the theoretical curve on Figure 8 is an average of 5 computations where the point source was placed at -16.7, -8.3, 0, 8.3 and 16.7 cm along the y axis ($y = 0$ cm stands for the center of the PC-based barrier front side, see Figure 4). Predictions and measurements present an overall agreement especially above 2500 Hz although the simulation process considers an array of infinite cylinders along the vertical dimension z. Both measured and predicted IL show the two band gaps (BG 0° and ABG) with similar width and attenuation. However, there is no amplification due to the negative refraction for the predicted IL and this effect appears around 2200 Hz only for the measured IL. This difference comes from the average over the 5 point sources and their position.

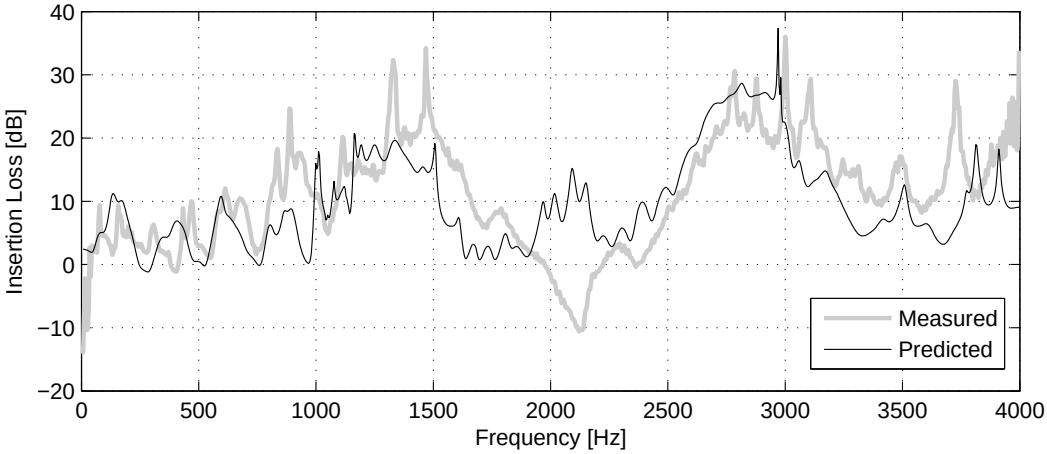

Figure 8 – Measured and theoretical (predicted through finite element code) Insertion Loss (IL) introduced by the PC-based noise barrier.

5. PERCEPTUAL ANALYSIS

5.1 Databases

To quantify the influence of a phononic crystal on the timbre of a sound source, the impulse responses obtained in Sections 3 and 4 are convoluted with 22 third-octave band white noise and 4 wideband signals (0 Hz to 4000 Hz). The central frequency of the noise corresponds to third octave between 25 Hz and 3150 Hz. Overall, the database includes 684 sound signals. The third-octave band white noises enable a detailed analysis of the frequency modifications introduced by the PC-based barrier whereas the wideband signals are employed to compare the three situations: free-field, PC-based barrier and free-standing barrier.

5.2 Psychoacoustic features

Since a PC introduces both a spectrum and a temporal modifications we employed a temporal quality parameter, the reverberation time at 60 dB, T_{60} (here given in ms). This parameter is estimated from the impulse responses obtained from the numerical computations and the acoustical measurements. It corresponds to the time for the sound level to decrease by 60 dB after the sound source ceases and quantifies thus the multiple reflections in the PC. Figure 9 shows the reverberation time estimated for the 10 predicted sound scenes and the 15 third-octave bands with central frequencies 125 Hz to 3150 Hz. The reverberation time decreases with the central frequency for all sound scenes. For the sound scenes 3 to 6, the reverberation time increases for the third-octave band with the central frequency 1000 Hz, corresponding to a gray zone in Figure 9. This effect is exacerbated for sound scene 5 at 1250 Hz, i.e. with a deeper PC-based barrier. Similar results are observed for reverberation times estimated from the acoustical measurements. The PC-based barrier introduces thus a significant temporal modification (i.e. a lower celerity) in the first band gap.

To check the audibility of the spectrum modification in the two band gaps (BG,0° and ABG), the loudness (perceived level) of the 684 signals has been estimated using the Zwicker model (18). This model takes into account the frequency masking effect and is optimized for signals with a continuous level such as the third-octave band white noises. The sound pressure level at the pseudo-listener is fixed to $L_p = 66\,\mathrm{dB_{SPL}}$ for the third-octave band of central frequency $f_c = 1000\,\mathrm{Hz}$ in free-field condition (sound scene 1). Several speech signals were considered in the databases: 4 talkers (2 males and 2 females) and 4 sentences per talker, an environmental sound signal and a musical recording (with percussive sounds). Figure 10 shows the estimated loudness of the 16 speech signals for the sound scenes 1 (free-field), 4 (PC-based barrier) and 8 (free-standing barrier), i.e. with the same position of the sound source and the same depth ($d = 0.5\,\mathrm{m}$) and width ($w = 2.35\,\mathrm{m}$) of the two barriers. We observe that the overall loudness is attenuated when a noise barrier is introduced between the sound source and the listener. Even though this attenuation appears for both PC-based and free-standing barriers, the loudness is two times higher with the PC-based noise barrier compared to the free-standing barrier. However, speech signal is wideband and the PC-based noise barrier used in this study was not designed for the attenuation of wideband signals.

Figure 11 shows the estimated loudness (at the right ear of the pseudo-listener) of the 14 third-octave band white noises with central frequencies 160 Hz to 3150 Hz for the 10 sound scenes. We observe a clear attenuation of the loudness for the sound scenes 7 to 10, i.e. when the free-standing noise barrier is placed between the sound source and the listener. The loudness is the lowest when the sound source is very close to

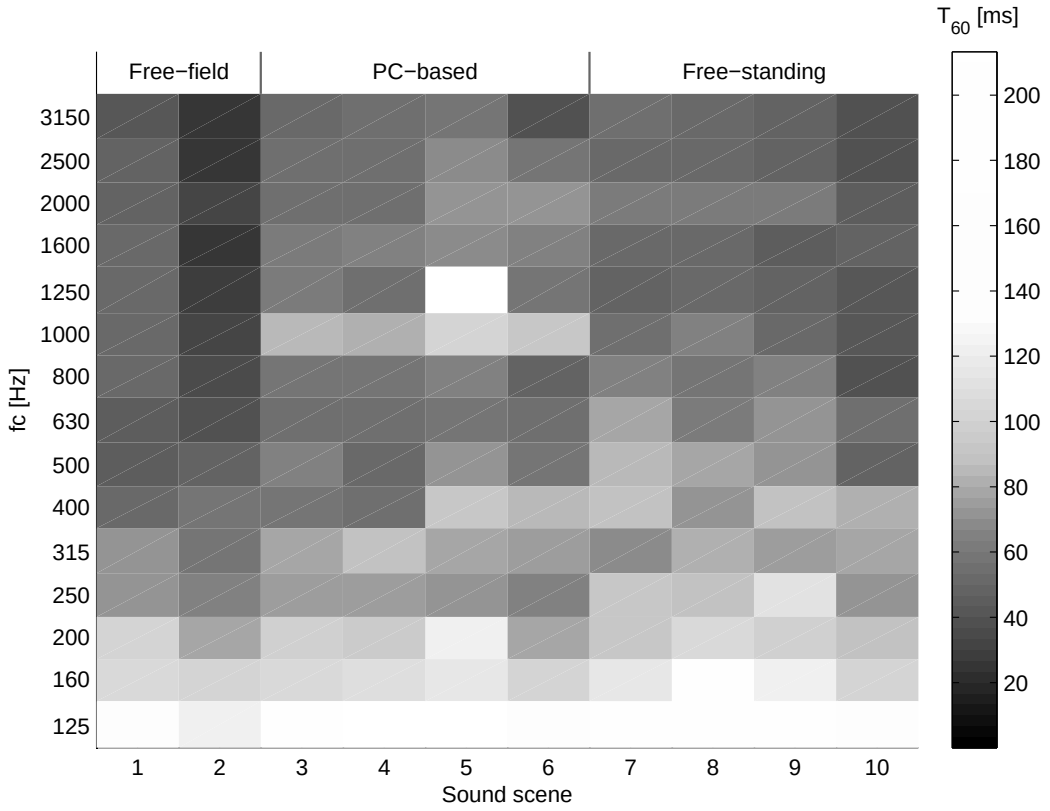

Figure 9 – Estimated reverberation time T_{60} of the third-octave band white noises with central frequencies 125 Hz to 3150 Hz for the 10 sound scenes listed in Table 1.

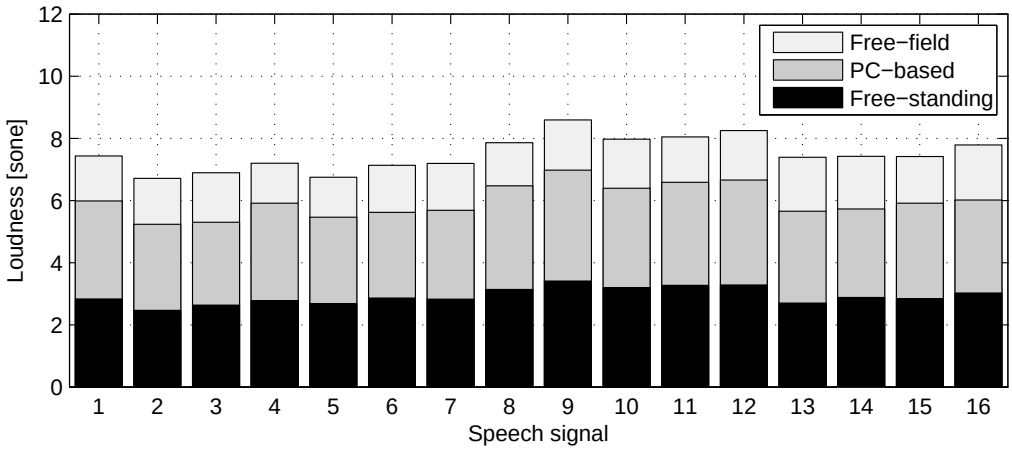

Figure 10 – Estimated loudness at the right ear of the pseudo-listener of the 16 speech signals for the three sound scenes 1 (free-field), 4 (PC-based barrier) and 8 (free-standing barrier), see Table 1.

the free-standing barrier (sound scene 10) and for frequencies above 1000 Hz. The loudness is higher with a PC-based barrier except for the frequencies near 1250 Hz (sound scenes 3 to 6, corresponding to the two band gap BG 0°) and 3150 Hz (sound scenes 3 to 5, ABG) where both barriers show the same attenuation. For the sound scene 6, the loudness increases compared to the reference scene (in this case sound scene 2) for frequencies near 2000 Hz. A noise barrier made of this specific phononic crystal enables a noise control equivalent to a free-standing noise barrier for frequencies close to the band gaps and introduce an artificial amplification of the loudness for a specific frequency band due the negative refraction: this is the focusing phenomenon.

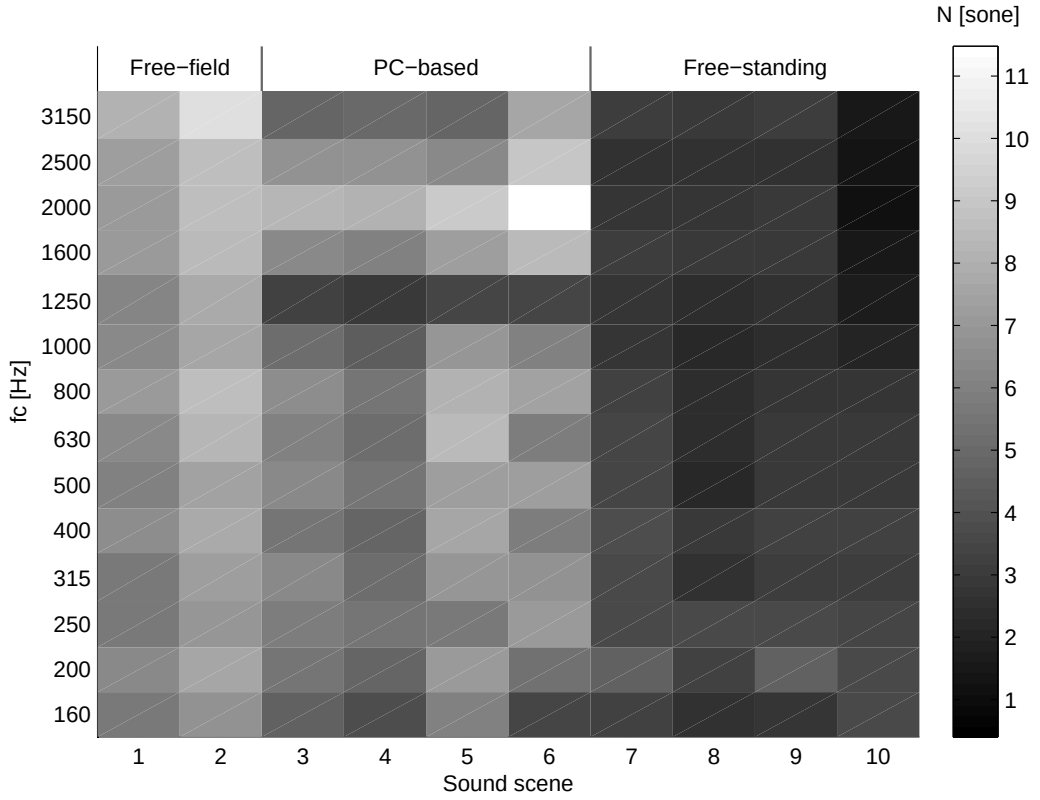

Figure 11 – Estimated loudness at the right ear of the pseudo-listener of the 14 third-octave band white noises with central frequencies 160 Hz to 3150 Hz for the 10 sound scenes of Table 1.

6. CONCLUSION

The phononic crystal designed for this study presents three different characteristics in the audible frequency range: a first band gap at normal incidence in the frequency range 1080 Hz to 1610 Hz, negative refraction in the range 1610 Hz to 2500 Hz, and an absolute band gap in the range 2500 Hz to 2960 Hz. These three effects are observed either in simulations with a finite element method and in an experiment with a demonstrator of a PC-based noise barrier. The perceptual analysis shows that a noise barrier made of a PC is able to attenuate the loudness of a noise source in the band gaps in the same level as a usual free-standing noise barrier. In addition to the spectral modification, a temporal modification is also introduced by the PC in these frequency bands. A focusing phenomenon introduces an increase of the loudness for a specific frequency band, around 2000 Hz for this PC. This phenomenon creates an image of the sound source behind the noise barrier, i.e. on the resident side. Its seems that focusing phenomenon is detrimental for noise control applications of PCs.

However, auditory tests are required to quantify the auditory impact of a PC. In a first test, we will ask the test subjects to compare the loudness and the timbre of different types of signals (narrow-band and wideband signals) for the sound scene listed in Table 1. Then, in a second test, we will quantify more precisely the impact of the negative refraction on the perceived distance of sound source.

ACKNOWLEDGEMENTS

We would like to thanks Gérard Haw and Romain Thery for their help during the manufacturing process of the phononic crystal structure.

REFERENCES

1. Marquis-favre C, Premat E, Aubrée D, Vallet M. Noise and its Effects - A Review on Qualitative Aspects of Sound. Part I: Notions and Acoustic Ratings. Acta Acustica United with Acustica. 2005;91:613–625.
2. European Parliament and Council. Directive 2002/49/EC of the European Parliament and of the Council of 25 June 2002 Relating to the Assessment and Management of Environmental Noise. Official Journal. 2002;189:12–26.
3. Watts GR. Acoustic performance of parallel traffic noise barriers. Applied Acoustics. 1996 Feb;47(2):95–119.
4. Arenas JP. Potential Problems with Environmental Sound Barriers when Used in Mitigating Surface Transportation Noise. Science of the Total Environment. 2008 Nov;405(1–3):173–179.
5. Sigalas MM, Economou EN. Attenuation of multiple-scattered sound. EPL (Europhysics Letters). 1996;36(4):241–246.
6. Sánchez-Pérez JV, Caballero D, Martinez-Sala R, Rubio C, Sanchez-Dehesa J, Meseguer F, et al. Sound Attenuation by a two-dimensional Array of Rigid Cylinders. Physical Review Letters. 1998;80(24):5325–5328.
7. Vasseur JO, Deymier PA, Khelif A, Lambin P, Djafari-Rouhani B, Akjouj A, et al. Phononic Crystal with Low Filling Fraction and Absolute Acoustic Band Gap in the Audible Frequency Aange: A Theoretical and Experimental Study. Physical Review E. 2002;65:056608.
8. Goffaux C, Maseri F, Vasseur JO, Djafari-Rouhani B, Lambin P. Measurements and calculations of the sound attenuation by a phononic band gap structure suitable for an insulating partition application. Applied Physics Letters. 2003 Jul;83(2):281–283.
9. Romero-Garcia V, Castiñeira-Ibañez S, Sanchez-Perez JV, Garcia-Raffi LM. Design of Wideband Attenuation Devices Based on Sonic Crystals made of Multi-Phenomena Scatterers. In: Proceedings of the Acoustics 2012 Nantes Conference. April; 2012. p. 283–288.
10. Koussa F, Defrance J, Jean P, Blanc-Benon P. Transport Noise reduction by low height sonic crystal noise barriers. In: Proceedings of the Acoustics 2012 Nantes Conference. April; 2012. p. 997–1001.
11. Lagarrigue C, Groby JP, Tournat V. Sustainable Sonic Crystal Made of Resonating Bamboo Rods. J Acoust Soc Am. 2013 Jan;133(1):247–254.
12. Sukhovich A, Merheb B, Muralidharan K, Vasseur JO, Pennec Y, Deymier PA, et al. Experimental and theoretical evidence for subwavelength imaging in phononic crystals. Phys Rev Lett. 2009;102:154301.
13. Hladky-Hennion AC, Vasseur JO, Haw G, Croënne C, Haumesser L, Norris AN. Negative refraction of acoustic waves using a foam-like metallic structure. Applied Physics Letters. 2013 April;102(14):144103.
14. Spiousas I, Etchemendy PE, Calcagno ER, Eguia MC. Shifts in the Judgement of Distance to a Sound Source in the Presence of a Sonic Crystal. In: Proceedings of Meetings on Acoustics. vol. 19; 2013. p. 050162.
15. ATILA, Finite-Element Software Package for the analysis of 2D & 3D structures based on smart materials. Lille, FR; 2010. Version 6.0.2.
16. Langlet P, Hladky-Hennion AC, Decarpigny JN. Analysis of the propagation of acoustic waves in passive periodic materials using the finite element method. J Acoust Soc Am. 1995;98:2792–2800.
17. ITU–T Rec P 58. Head and Torso Simulator for Telephonometry. CH–Geneva; 1996. International Telecommunication Union.
18. Fastl H, Zwicker E. Psychoacoustics: Facts and models. 3rd ed. DE–Berlin: Springer; 1990.